

SPATIAL DISTRIBUTION OF CHLOROPHYLL *a* AND PHAEOPIGMENTS *a* AND THE RELATIONSHIPS WITH ZOOPLANKTON COMMUNITY IN THE WESTERN BLACK SEA

DAN VASILIU¹, MIHAELA MURESAN¹, DAN SECRIERU¹, SORIN BALAN¹, ANDRA BUCSE²

¹National Institute of Marine Geology and Geo-Ecology (GeoEcoMar), 23-25 Dimitrie Onciul St., 024053 Bucharest, Romania

²University Ovidius, Faculty of Applied Sciences and Engineering, 124 Mamaia Blvd., 900527, Constanta, Romania

Abstract. Chlorophyll *a* (Chl *a*) and phaeopigments *a* (Phaeo *a*) spatial distribution in the Western Black Sea was studied in relation to environmental factors and mesozooplankton community. For that purpose, CTD parameters, nutrients, chlorophyll pigments, and mesozooplankton total density and biomass were measured at 33 stations, distributed along the Romanian shelf waters, in June 2016. The studied area was divided into 4 subareas (NIS – northern inner shelf, NOS – northern outer shelf, SIS – southern inner shelf, and SOS – southern outer shelf). The hydrological regime, characterized by large Danube's flow and a coastal upwelling phenomenon observed both in the NIS and SIS, strongly influenced the spatial variability of Chl *a* and Phaeo *a*. Surface Chl *a* and Phaeo *a* showed the highest concentrations within NIS, followed by NOS, both subareas subjected to larger freshwater input from the Danube River. The vertical distribution of Chl *a* in the inner shelf waters generally showed a subsurface maximum layer within 6–24 m (the shallower and stronger ones within NIS). The outer shelf waters displayed two subsurface maxima; an upper one (within 7–20 m) and a deeper one, slightly higher than the upper one, observed both in NOS and SOS at 30–45 m depth. Phaeo *a* showed relatively similar vertical profiles to Chl *a*, with a subsurface maximum generally coinciding with subsurface chlorophyll maximum. The meroplankton showed positive correlations with the chlorophyll pigments, which suggest a strong link between pigments abundances and distribution and development and production of larvae in the coastal waters.

Key words: Western Black Sea; Danube River; chlorophyll *a*; pheopigments *a*; zooplankton

1. INTRODUCTION

Chlorophyll *a* (Chl *a*), through its unique photosynthetic function, has been accepted for over 60 years as the proxy to estimate the algal biomass and primary productivity in the aquatic environment due to its easy, fast and highly precise analytical methods. An ubiquitous phenomenon in marine waters is the presence of deep chlorophyll maximum layer. Its formation and maintenance has been extensively studied since the 1950s; a variety of different explanations have been provided, including the accumulation of cells at a pycnocline or behavioral aggregation of motile cells (ex. dinoflagellates) as a defense against grazing (Hanson *et al.*, 2007). However, the deep chlorophyll maximum can be seen not only as a consequence of the increase in biomass, but also as a physiological adaptation of phytoplankton to low light levels (Cullen, 1982).

The main Chl *a* degradation products, namely phaeophorbide *a* and phaeophytin *a* (together commonly known as phaeopigments *a*), are considered as indicators of grazing activity (Jeffrey, 1980). However, while phaeophorbide *a* is usually considered as a degradation product of Chl *a* issued from grazing, phaeophytin *a* can also be due to senescence (Taguchi *et al.*, 1993). In spite of numerous Chl *a* degradation pathways (Yentsch, 1965; Wolken *et al.*, 1955), it is widely recognized that the main source of chlorophyll break-down products in aquatic environments is in fecal materials resulting from the grazing pressure (Lorenzen, 1967; Jeffrey, 1980; Taguchi *et al.*, 1993). The spatial distribution of phaeopigments in natural waters is linked not only to their production, but also to their photo-degradation (Soo-Hoo & Kiefer, 1982), thus, the concentration of phaeopigments at a given depth results from a balance between local rates of grazing and rates of photooxidation (Soo-Hoo & Kiefer, 1982).

The spatial distribution of Chl *a* has been well documented in the Western Black Sea since the mid-1970s (Bologa, 1977; Bologa *et al.*, 1985; Vasiliu, 2010b; Yunev, 1989), especially considering the dramatic direct effects of the intense eutrophication during 1980–1990. The studies approaching that period were dealt especially with the surface Chl *a* and phytoplankton (Mihnea, 1988, 1997; Velikova *et al.*, 2005; Demidov, 2008; Yunev *et al.*, 2007; Vasiliu *et al.*, 2012a); quite less attention was paid to chlorophyll and phytoplankton vertical profiles. However, starting with the late 1990s, the studies concerning Chl *a* vertical distribution in the Western Black Sea, particularly the occurrence of deep chlorophyll maximum and its relationships with primary productivity, have intensified (Yunev *et al.*, 2005; Chu *et al.*, 2005; Vasiliu *et al.*, 2010a).

Unlike chlorophyll, the studies related to phaeopigments have been rather sporadic in the Western Black Sea area (particularly the Romanian Black Sea shelf waters), even if they have started since the mid-1970s (Bologa, 1978). Phaeopigments were initially measured only for obtaining accurate chlorophyll estimates, since these relatively common compounds have absorption and emission spectra similar to that of chlorophyll (Lorenzen, 1967). Since the 1990s, the studies of chlorophyll degradation products and its relationships with the plankton community have intensified (Yunev, 1989; Krupatkina *et al.*, 1991; Mihnea, 1997), but they have still remained relatively few. Evidences about the

strong relation between the phytoplankton blooms and zooplankton composition and abundance distribution in the Black Sea were brought out by several authors (Stel'makh *et al.*, 2009; Stefanova *et al.*, 2012).

The present work aims to analyze the spatial distribution of chlorophyll *a* and some of its breakdown products (phaeophytin *a* and phaeophorbide *a*) along the Romanian Black Sea shelf waters, under highly variable hydrological conditions, and the factors controlling their variability. Its relationship with zooplankton spatial distribution and abundance was demonstrated.

2. MATERIALS AND METHODS

2.1. SAMPLING AREA

30 stations, covering the Romanian shelf waters (Western Black Sea), were sampled during the research cruise aboard R/V *Mare Nigrum* conducted in June 2016. The studied area was divided into 4 subareas, as follows: northern inner shelf (NIS), northern outer shelf (NOS), southern inner shelf (SIS) and southern outer shelf (SOS). The inner shelf areas included stations with bottom depths <60 m and the outer shelf areas – stations with bottom depths within 60-200 m.

The Figure 1 shows the four subareas included within the studied area, while the Table 1 shows the sampling stations included within each subareas.

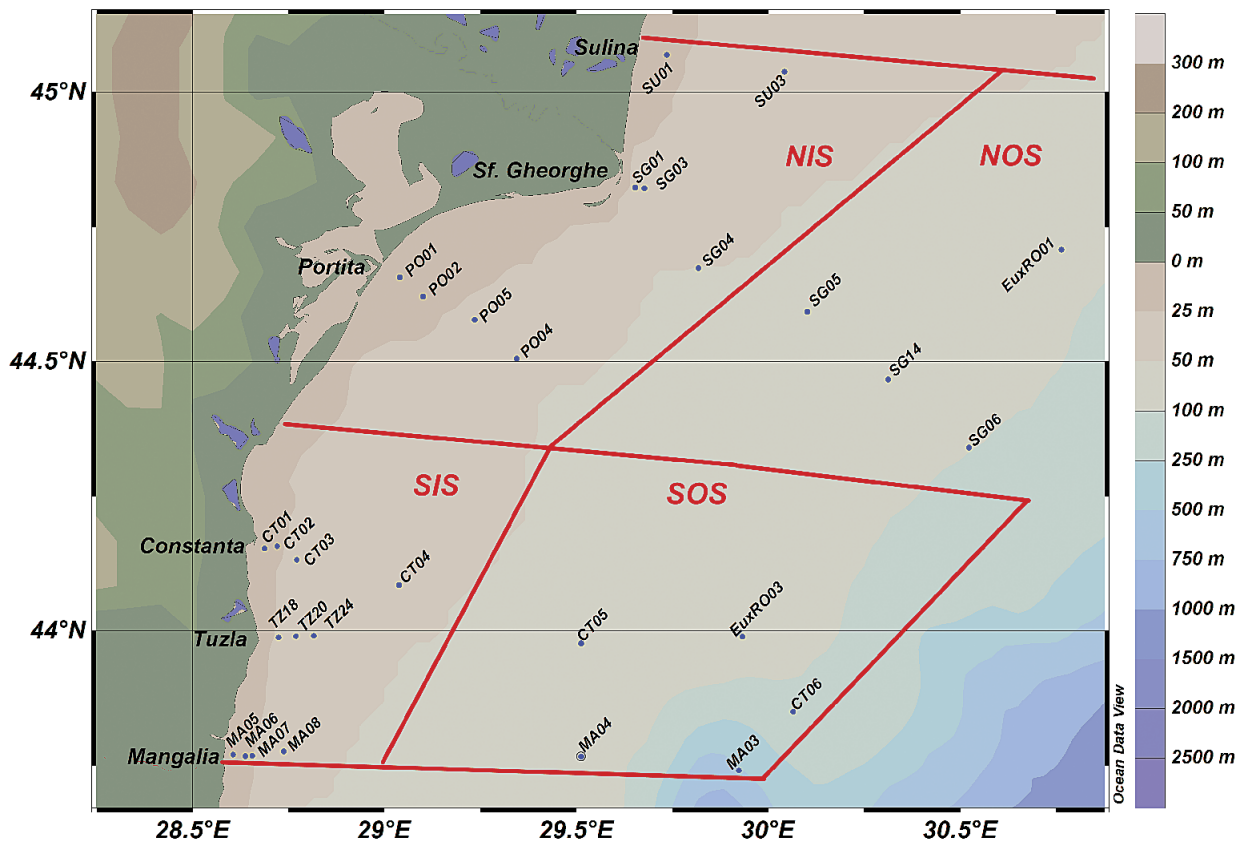


Fig. 1. Sampling area (Black Sea Romanian shelf waters)

Table 1. List of sampling stations

Subarea	Sampling station	Coordinates	Bottom depth, m
NIS	SU01	45.0698 N; 29.7356 E	15.0
	SU03	45.0385 N; 30.0421 E	34.6
	SG01	44.8229 N; 29.6532 E	23.7
	SG03	44.8215 N; 29.6772 E	37.5
	SG04	44.6733 N; 29.8174 E	52.4
	P001	44.6568 N; 29.0399 E	13.5
	P002	44.6209 N; 29.1000 E	20.3
	P004	44.5052 N; 29.3443 E	42.8
	P005	44.5776 N; 29.2355 E	30.2
NOS	SG05	44.5919 N; 30.1011 E	63.6
	SG14	44.4663 N; 30.3116 E	76.2
	SG06	44.3399 N; 30.5228 E	92.8
	EuxR001	44.7077 N; 30.7632 E	79.2
SIS	CT01	44.1530 N; 28.6880 E	16.2
	CT02	44.1571 N; 28.7206 E	27.0
	CT03	44.1315 N; 28.7718 E	33.0
	CT04	44.0847 N; 28.0377 E	46.0
	TZ18	43.9880 N; 28.7245 E	33.8
	TZ20	43.9897 N; 28.7698 E	38.6
	TZ24	43.9907 N; 28.8154 E	42.8
	MA05	43.7696 N; 28.6061 E	16.8
	MA06	43.7667 N; 28.6367 E	26.5
	MA07	43.7679 N; 28.6560 E	35.0
	MA08	43.7756 N; 28.6560 E	44.6
SOS	CT05	43.9764 N; 29.5126 E	63.8
	CT06	43.8496 N; 30.0640 E	87.7
	EuxR003	43.9892 N; 29.9326 E	74.6
	MA04	43.7663 N; 29.5127 E	67.0
	MA03	43.7406 N; 29.9228 E	85.0

2.2. ANALYTICAL PROCEDURES

Vertical profiles of temperature, salinity, dissolved oxygen (DO), and fluorescence were obtained using a SBE 25 CTD. The raw CTD data were binned and averaged every 1 dbar from the surface to ≈ 5 –10 m above seafloor. For this study, we use only measurements made during the downcast.

Water samples for nutrients, chlorophyll *a*, and phaeopigments *a* analyses were collected with a Sea Bird SBE 32 carousel water sampler (12 Niskin bottles, 5 L each), attached to the SBE 25, on the upcast, at different depths selected according to the CTD vertical profiles.

Nutrients (phosphate, silicate, nitrite, nitrate, and ammonium) were measured by spectrometry (UV-VIS Perkin Elmer

Lambda 35 spectrophotometer) following the standard seawater methods (Grasshoff *et al.*, 1999).

Water samples for chlorophyll *a* and phaeopigments *a* analyses were filtered onboard through Millipore nitrocellulose membrane (porosity of 0.8 μm), the filters being then immediately frozen at -50°C until the subsequent analyses. Pigments were extracted with 90% acetone from the homogenate filter and determined by spectrometry according to the monochromatic equations of Lorenzen (1967). For phaeopigments *a* measurements, the centrifuged extracts were acidified with HCl 1% for 2–3 minutes before readings. The acidification techniques used to measure phaeopigments by spectrometry do not distinguish between phaeophytin *a* and phaeophorbide *a* (Aminot & Rey, 2001).

All parameters were processed and displayed using Ocean Data View (ODV) software, version 4.7.10 (Schlitzer, 2017).

28 samples of mesozooplankton were collected by means of a Juday net (38 cm opening, 150 µm mesh size). The net was vertically towed from the water bottom depth up to the surface, thus the integral water column being sampled. On board the samples were immediately preserved with 4% buffered formalin and stored in jars. The samples processing and analysis in the laboratory were done according to Alexandrov *et al.* (2014).

2.3. STATISTICAL ANALYSIS

Statistical data processing was done using the program XLSTAT 7.5.2. The non-parametric test Kruskal-Wallis (K-W) was employed to test the differences between subareas for given variables, because of the non-normal distribution of all variables considered which resulted from applying the normality test Shapiro-Wilk at the level of significance $\alpha=0.05$. The K-W test is a non-parametric equivalent to one-way ANOVA by ranks, testing the null hypothesis that 3 or more groups all come from the same distribution. The Mann-Whitney significance test was applied to analyze the differences between every pair of groups. In order to investigate the factors influencing the spatial variability of Chl *a* and Phaeo *a*, the relationships between physical-chemical and biological variables were tested after log transformation of all variables that did not comply with the assumption of normality. The Kendall tau's ranks correlation coefficient was also used for testing correlations between different zooplankton taxa with chlorophyll pigments. All statistical analyses were carried out to the significance level of $\alpha=0.05$.

3. RESULTS

3.1. HYDROGRAPHIC CONDITIONS

Sea Surface Temperature (SST) and Sea Surface Salinity (SSS) ranged within 15.86–26.46°C (mean of 21.27°C; standard deviation of 2.44°C) and 8.03–17.77 PSU (mean of 14.85

PSU; standard deviation of 2.74 PSU), respectively. The K-W tests applied for variables SST and SSS displayed significant differences between subareas ($p=0.02$ and $p=0.0002$, respectively).

SST showed significant higher values in the outer shelf waters as against the inner shelf waters. No significant differences between NIS and SIS were observed (Table 2), in connection with the coastal upwelling phenomenon observed either in the shallower southernmost waters or Portita bay (Fig. 2).

Significant higher SSSs were found in the southern shelf waters (Fig. 2), both SIS and SOS, while the lowest SSSs were measured within either NIS or NOS (Table 2). The absence of any significant differences between SIS and SOS and, on the other hand, NIS and NOS is due to the coastal upwelling phenomenon. Generally, the salinity regime in NIS is stronger influenced by the Danube's freshwater discharge than NOS, but the more saline upwelled waters in the Portita bay led to relatively closed medians corresponding to the concerned two subareas (13.92 PSU and 13.96 PSU, respectively). Similarly, the lack of any significant differences between SIS and SOS in terms of SSS can be explained.

The large Danube's freshwater discharges, associated with the upwelling phenomenon led to weaker water masses stratification in the Romanian shelf waters. An upper mixed layer with maximum thickness of 8 m was observed at sampling stations with bottom depths varying between 43 m and 67 m (MA04, CT04, CT05, PO04, and SG05). Shallower stations showed a very thin upper layer (up to 5 m depth) characterized either by low salinities, within NIS (in the Danube's direct influence area – PO05, SG01, SG03, SG04, SU01, and SU03) or high salinities and low temperatures, within SIS (influence of upwelling phenomenon – MA05, MA06, MA07, and MA08) (Figs. 3 and 4). The deeper stations, both in NOS and SOS, showed a very thin upper layer as well (even thinner – up to 3 m depth at stations SG06 and MA03) (Figs. 3 and 4), most

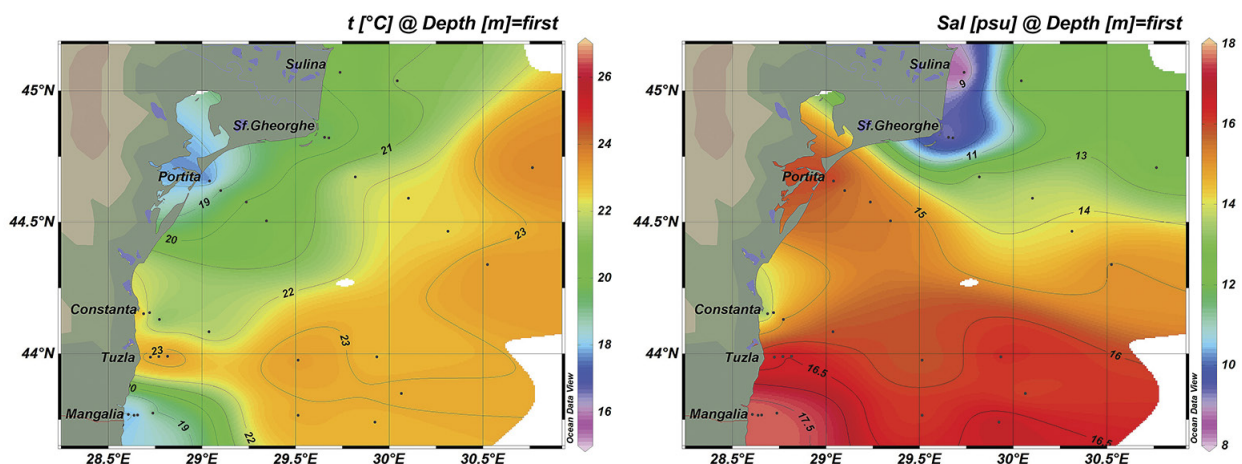


Fig. 2. Sea Surface Temperature (SST) and Salinity (SSS) in the studied area

Table 2. Mann-Whitney significance tests between subareas in terms of SST, SSS, and surface DO

		NIS	NOS	SIS	SOS
NIS	SST		0.005		0.0001
	SSS			0.001	0.003
	Surface DO			0.017	0.0002
NOS	SST	>			
	SSS			0.011	0.004
	Surface DO				0.006
SIS	SST				0.017
	SSS	>	>		
	Surface DO	<			0.0002
SOS	SST	>		>	
	SSS	>	>		
	Surface DO	<	<	<	

Note: Upper right values represent the level of significance (p); the absence of p values shows not significant differences between subareas. Lower left symbols compare subareas in the first column with subareas in the first row.

probable in connection with higher freshwater discharges of the Chilia arm and upwelling event (Mangalia area).

3.2. DISSOLVED OXYGEN (DO) AND NUTRIENTS

Overall, DO ranged within 1.66–12.35 mg·L⁻¹ with maximum at station SG03, in the surface layer, and minimum at station CT06, in the bottom layer (~80 m depth). The surface DO showed a relatively large spatial variability (Fig. 5), varying from 7.17 mg·L⁻¹ (CT06) and 12.35 mg·L⁻¹ (SG03). The K-W test applied to surface DO concentration showed significant differences between subareas (p<0.0001). Thus, the surface DO showed the highest concentrations within NIS and NOS, in connection with larger Danube's discharge (Table 2), while the lowest ones were observed within SOS (none of the concentrations exceeded 8.0 mg/l).

DO vertical distribution in the inner shelf waters generally showed a gradual decrease from the surface (8.24–12.35 mg/l) to bottom layers (4.19–7.70 mg·L⁻¹) without exhibiting a subsurface maximum (excepting for SG04 – Fig. 6). Some stations within SIS (MA08, TZ18, TZ20, and TZ24) showed weak DO subsurface maxima (8.55–9.34 mg/l) at depths ranging within 12–18 m (Fig. 6). The outer shelf waters (both NOS and SOS) showed well pronounced DO maxima (8.90–9.92 mg·L⁻¹) at depths ranging within 17–24 m. The DO vertical profiles generally showed a strong oxycline starting from the depths of 60–72 m within NOS and 50–55 m within SOS, respectively (Fig. 6). The bottom DO concentrations ranged from 2.29 mg·L⁻¹ (SG06) to 6.85 mg/l (SG05) within NOS and from 1.66 mg·L⁻¹ (CT06) to 6.15 mg·L⁻¹ (CT05) within SOS, respectively.

Phosphate concentrations varied between values below detection limit and 2.72 µM (at station PO05, at water–sediment interface). The phosphate spatial distribution was relatively homogeneous either in the surface layer or at water–sediment interface (no significant differences between areas – K-W, p=0.61 and K-W, p=0.47, respectively). However, relatively high surface concentrations were measured at stations

located in front of Sfantu Gheorghe arm (0.73 µM–0.77 µM) (Fig. 7), while the water–sediment interface showed relatively high phosphate concentrations in the Portita area (PO04 – 0.72 µM and PO05 – 2.72 µM), near shore waters in the Mangalia area (MA05 – 1.26 µM and MA07 – 2.58 µM), probably in connection with the upwelling phenomenon, and, obviously, at deeper stations (SG06 – 1.064 µM, EuxRO01 – 0.82 µM, and CT06 – 0.94 µM).

Vertical profiles of phosphate showed higher concentrations in the upper layer, followed by a significant decrease within thermocline. Below thermocline, it can be observed an increase in the phosphate concentration up to their maximum at the water-sediment interface (0.08–2.72 µM). No significant differences were observed between subareas in terms of bottom PO₄ concentrations (K-W, p=0.473).

Silicates ranged from 0.94 µM (at station SG05, in the upper thermocline) to 51.11 µM (at station SG 01, at surface layer). The K-W test showed no significant differences between subareas in terms of surface silicate concentrations (p=0.089). However, higher surface concentrations were measured in front of Sfantu Gheorghe and Sulina arms (40.34–51.11 µM and 36.09 µM, respectively), but relatively increased silicates were also found in the very shallow waters nearest the shore, in front of Constanta harbour (CT01 – 10.96 µM) and in the Mangalia area (MA06 – 11.12 µM), the latter, most probable, linked to the coastal upwelling (Fig. 7). Nevertheless, despite of the surface silicates maxima recorded in front of the Danube's mouths, significant higher concentrations were recorded at the water–sediment interface as compared to the surface layer (M-W, p<0.0001).

As regarding the vertical distribution of silicate, their concentrations increased with depth up to the water–sediment interface, where the maxima were reached. The highest silicate concentrations at the water–sediment interface were measured at deeper stations within NOS (SG06 – 33.37 µM and EuxRO01 – 30.07 µM) and SOS (CT06 – 33.65 µM and

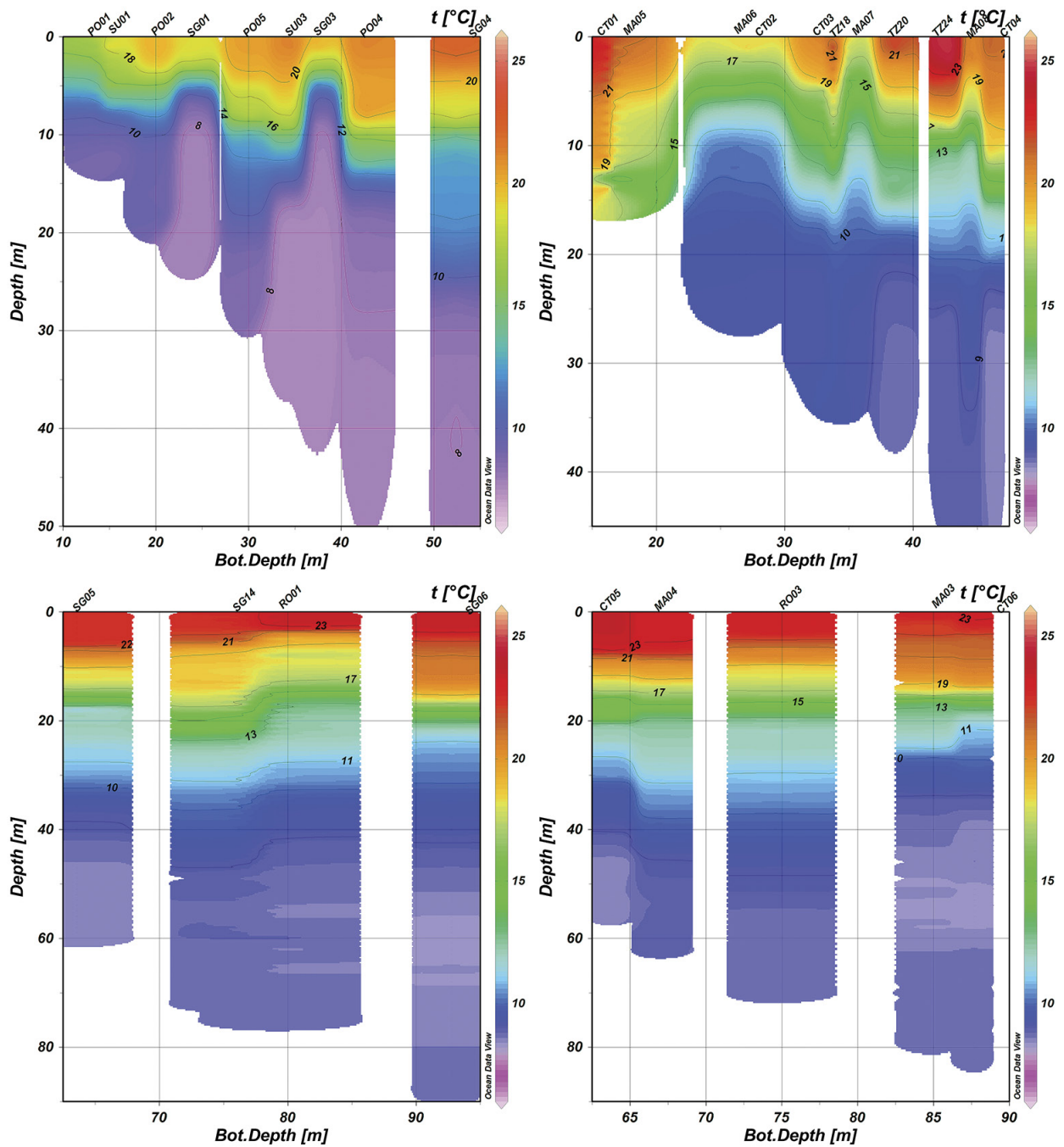
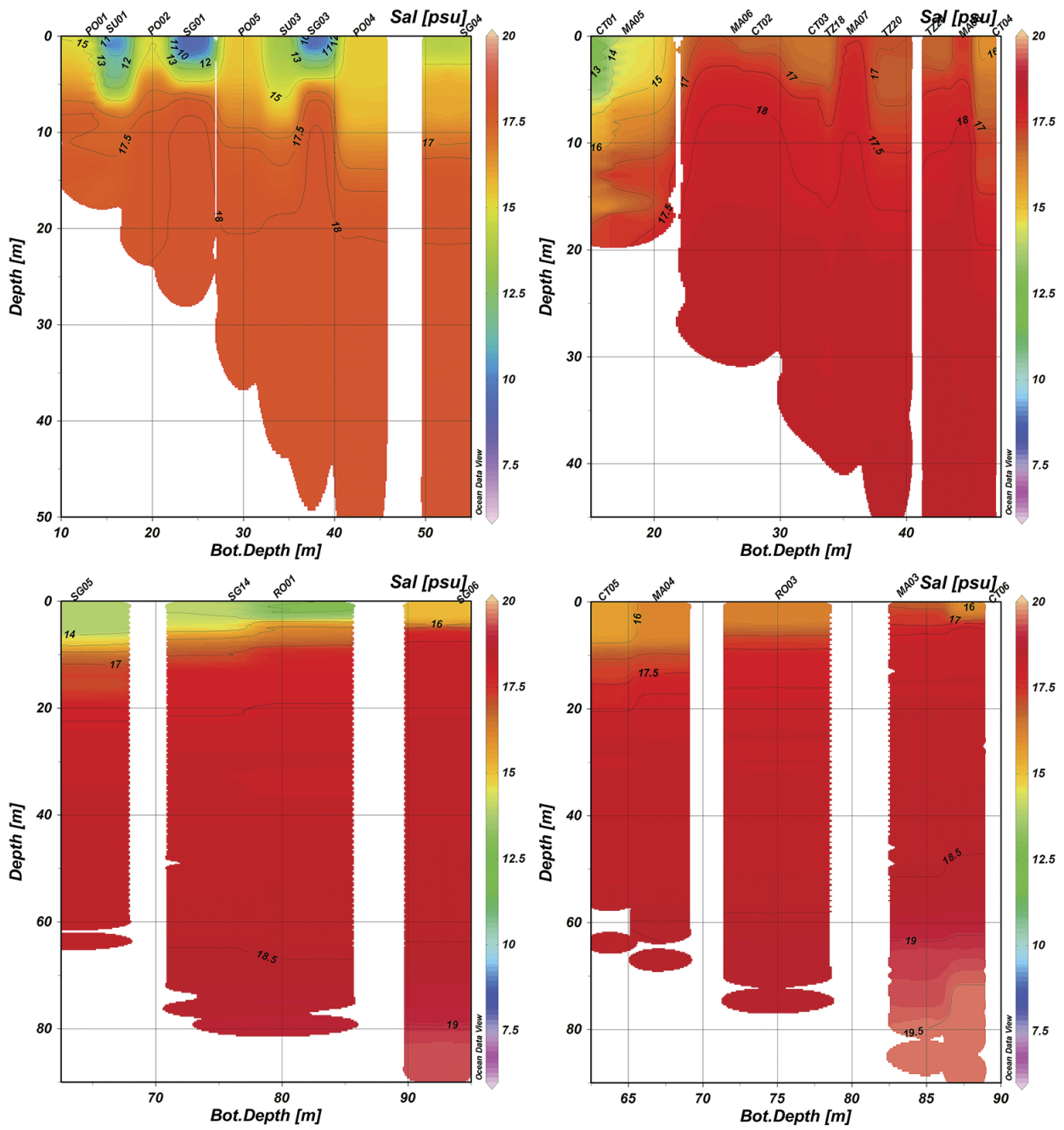
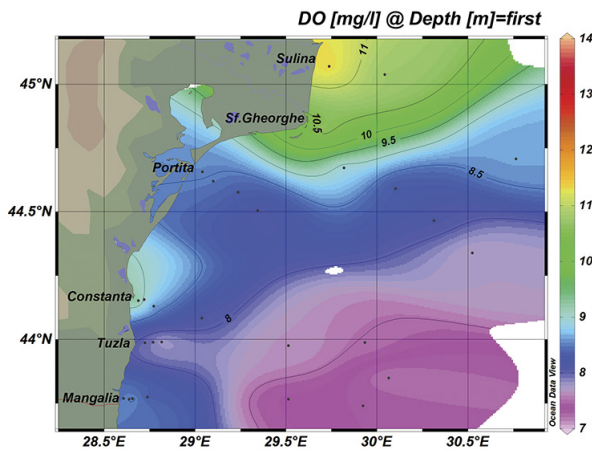


Fig. 3. Vertical distribution of temperature in the studied area (NIS-upper left; SIS-upper right; NOS-lower left; SOS-lower right)



▲ Fig. 4. Vertical distribution of salinity in the studied area (NIS-upper left; SIS-upper right; NOS-lower left; SOS-lower right)



◀ Fig. 5. Surface DO in the studied area

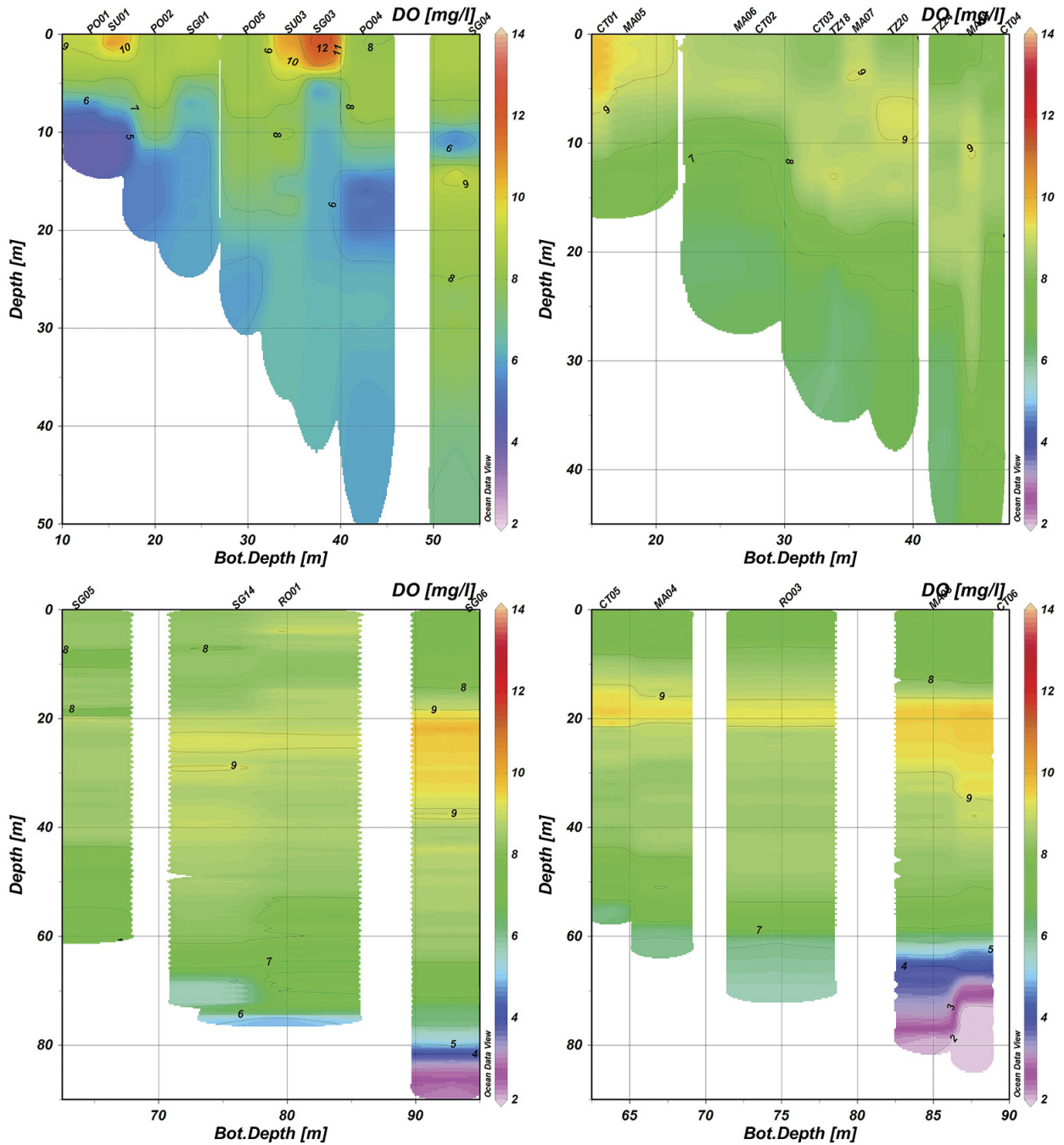


Fig. 6. Vertical distribution of DO in the studied area (NIS-upper left; SIS-upper right; NOS-lower left; SOS-lower right)

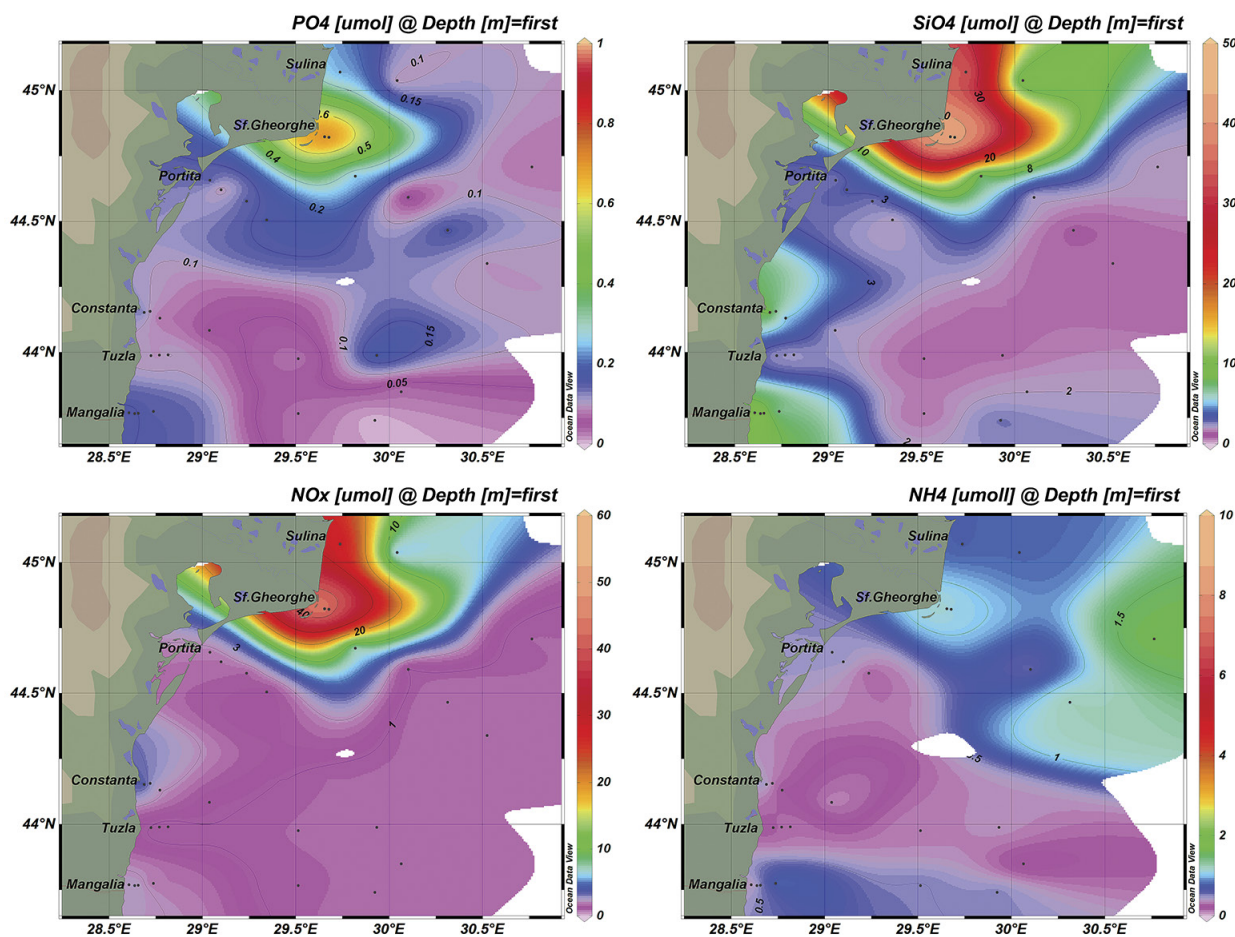


Fig. 7. Surface nutrients in the studied area

MA03 – 32.63 μM), but it can be remarked the relatively high concentrations in the Portita bay (20.20–27.74 μM), most probable as a result of intense remineralization process of the diatoms' frustules settled on the sediment top layer.

The oxidized form of inorganic nitrogen ($\text{NO}_x = \text{NO}_3^- + \text{NO}_2^-$) showed concentrations varying from 0.01 μM to 62.26 μM , with minimum at station SG05, in the surface layer and maximum at station SG 01, also in the surface layer. The K-W test applied for the variable surface NO_x showed no significant differences between subareas ($p=0.108$). However, similar to silicate, considerable higher surface NO_x concentrations were observed within NIS (Fig. 7), in front of the Danube mouths (SG01 – 62.26 μM , SG03 – 30.35 μM , and SU01 – 29.72 μM) in connection with the larger Danube's discharge, as suggested by the significant negative correlations between surface NO_x and SSS ($r=-0.736$, $p<0.0001$). Nevertheless, the lack of any significant differences between subareas is due to low surface NO_x concentrations found in the Portita bay (0.79–1.39 μM) which contribute to relatively close medians.

NO_x vertical distribution showed a weak maximum in the upper thermocline, at depths between 10 and 15 m, followed by a decrease down to below thermocline, where the concentrations started to increase again up to their maxima,

at the water–sediment interface, which ranged within 0.21–17.63 μM .

Ammonium concentrations varied between values below detection limit and 28.24 μM (at station MA05, at the water–sediment interface). Similar to other nutrients, the water–sediment interface showed ammonium concentrations significant higher than surface layer ($M-W$, $p=0.005$). The K-W test applied for the surface ammonium showed no significant differences between subareas ($p=0.182$). However, higher surface ammonium concentrations were observed in the northern part of the Romanian shelf waters, either in NOS (maximum of 1.61 μM , at station EuxRO01) or NIS (maxima of 1.57 μM and 1.66 μM at stations SG01 and SG03, respectively), while at water-sediment interface, higher ammonium concentrations were found in the near shore waters in the Mangalia area (MA05 – 28.24 μM).

3.3. CHLOROPHYLL A (CHL A) AND PHAEOPIGMENTS A (PHAE A)

Surface Chl *a* and Phaeo *a* displayed concentrations varying between 0.13 $\mu\text{g}\cdot\text{L}^{-1}$ and 17.25 $\mu\text{g}\cdot\text{L}^{-1}$ (Mean=3.06 $\mu\text{g}\cdot\text{L}^{-1}$; St-Dev=4.14 $\mu\text{g}\cdot\text{L}^{-1}$) and 0.20 $\mu\text{g}\cdot\text{L}^{-1}$ and 14.25 $\mu\text{g}\cdot\text{L}^{-1}$ (Mean=1.99 $\mu\text{g}\cdot\text{L}^{-1}$; StDev=3.09 $\mu\text{g}\cdot\text{L}^{-1}$), respectively. The K-W tests revealed

significant differences between subareas in terms of surface Chl *a* and Phaeo *a* ($p=0.003$ and $p=0.03$, respectively). The significant negative correlations between surface Chl *a* and SSS ($r=-0.77$, $p<0.0001$) and surface Phaeo *a* and SSS ($r=-0.88$, $p<0.0001$), respectively, suggest the strong influence of the Danube's discharge on the spatial distribution of pigments. The highest surface Chl *a* concentrations were measured in the Danube mouths area (SU01 – $17.25 \mu\text{g}\cdot\text{L}^{-1}$, SU3 – $6.57 \mu\text{g}\cdot\text{L}^{-1}$, SG01 – $7.07 \mu\text{g}\cdot\text{L}^{-1}$, and SG03 – $14.30 \mu\text{g}\cdot\text{L}^{-1}$) (Fig. 8), suggesting a strong algal bloom favoured by less saline, turbid and nutrient rich surface waters. However, the M-W tests applied for each pair of subareas showed significant higher surface

Chl *a* concentrations within NIS as compared to SIS, NOS and SOS and within NOS in comparison to SOS (Table 3). The M-W tests applied for the variable surface Phaeo *a* revealed also significant higher concentrations within NIS as compared to the southern shelf waters (both SIS and SOS – Table 3), but no significant differences between NIS and NOS. Similarly to Chl *a*, the surface Phaeo *a* showed the highest concentrations in the Danube's mouths area ($5.17-14.05 \mu\text{g}\cdot\text{L}^{-1}$) (Fig. 8), strongly linked to the intense phytoplankton development as well as *Noctiluca scintillans* degradation and high number of micrograzers such as meroplanktonic larvae of polychaets, bivalves and barnacles.

Table 3. Mann-Whitney significance tests between subareas in terms of surface Chl *a*, Phaeo *a*, $\text{Chl}_{\text{max}} a$, SCM depth and SPM depth

		NIS	NOS	SIS	SOS
NIS	Surface Chl <i>a</i>		0.014	0.001	0.003
	Surface Phaeo <i>a</i>			0.003	0.003
	SCM depth		0.024	0.016	0.009
	$\text{Chl}_{\text{max}} a$		0.025	0.028	0.008
	SPM depth		0.047		0.034
NOS	Surface Chl <i>a</i>	<			0.027
	Surface Phaeo <i>a</i>	>			
	SCM depth	>			
	$\text{Chl}_{\text{max}} a$	<			
	SPM depth	>			
SIS	Surface Chl <i>a</i>	<			
	Surface Phaeo <i>a</i>	<			
	SCM depth	>			
	$\text{Chl}_{\text{max}} a$	<			
	SPM depth	<			
SOS	Surface Chl <i>a</i>	<	<		
	Surface Phaeo <i>a</i>	<			
	SCM depth	>		>	
	$\text{Chl}_{\text{max}} a$	<			
	SPM depth	>			

Note: Upper right values represent the level of significance (p); the absence of p values shows not significant differences between subareas. Lower left symbols compare subareas in the first column with subareas in the first row.

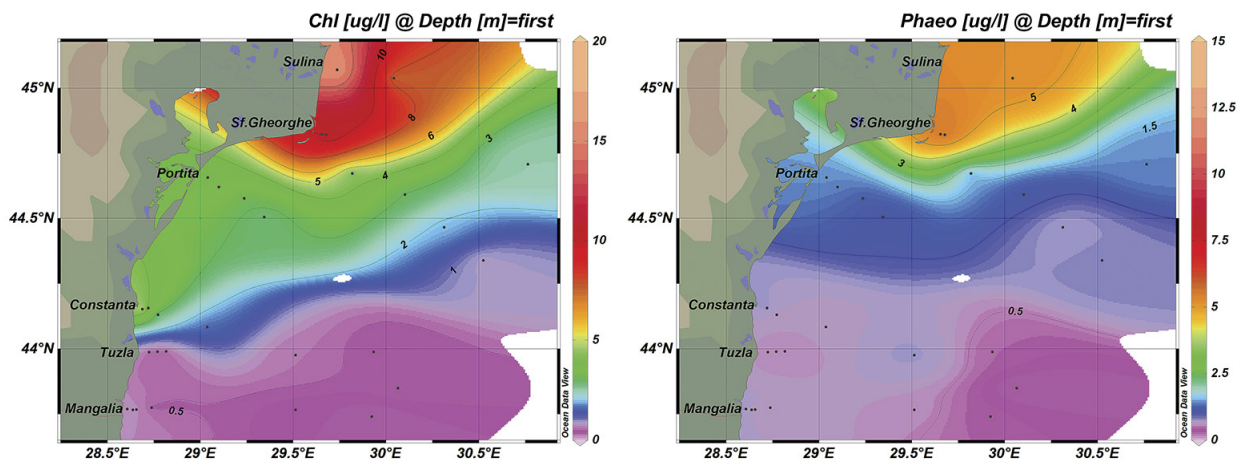


Fig. 8. Surface Chl *a* and Phaeo *a* in the studied area

CTD fluorescence vertical profiles showed generally quite well pronounced subsurface maxima. The inner shelf waters (excepting for the northernmost nearest shore station – SU01) showed one fluorescence maximum with depths ranging within 3–22 m (deeper in the Tuzla and Mangalia areas), while the outer shelf waters displayed generally two fluorescence maxima, an upper one having its core at 5–18 m depth and a lower one at 14–44 m depth (Fig. 9).

The *in situ* fluorescence intensities exhibited a significant positive correlation with the discrete chlorophyll *a* concentrations ($r=0.831$, $p<0.0001$), therefore the depth of the CTD

fluorescence maximum can be considered to be an effective proxy for the depth of the subsurface chlorophyll maximum (SCM). Nevertheless, this definition has one potential disadvantage: the reduction of the fluorescence signal in surface waters during the daylight hours around noon (Falkowski & Kolber, 1995), which can lead to false subsurface fluorescence maxima in daytime profiles. Though no significant relationship between surface fluorescence and time of day was found ($p=0.22$), the fluorometry-based definition of SCM was adopted in the present paper, considering the surface waters

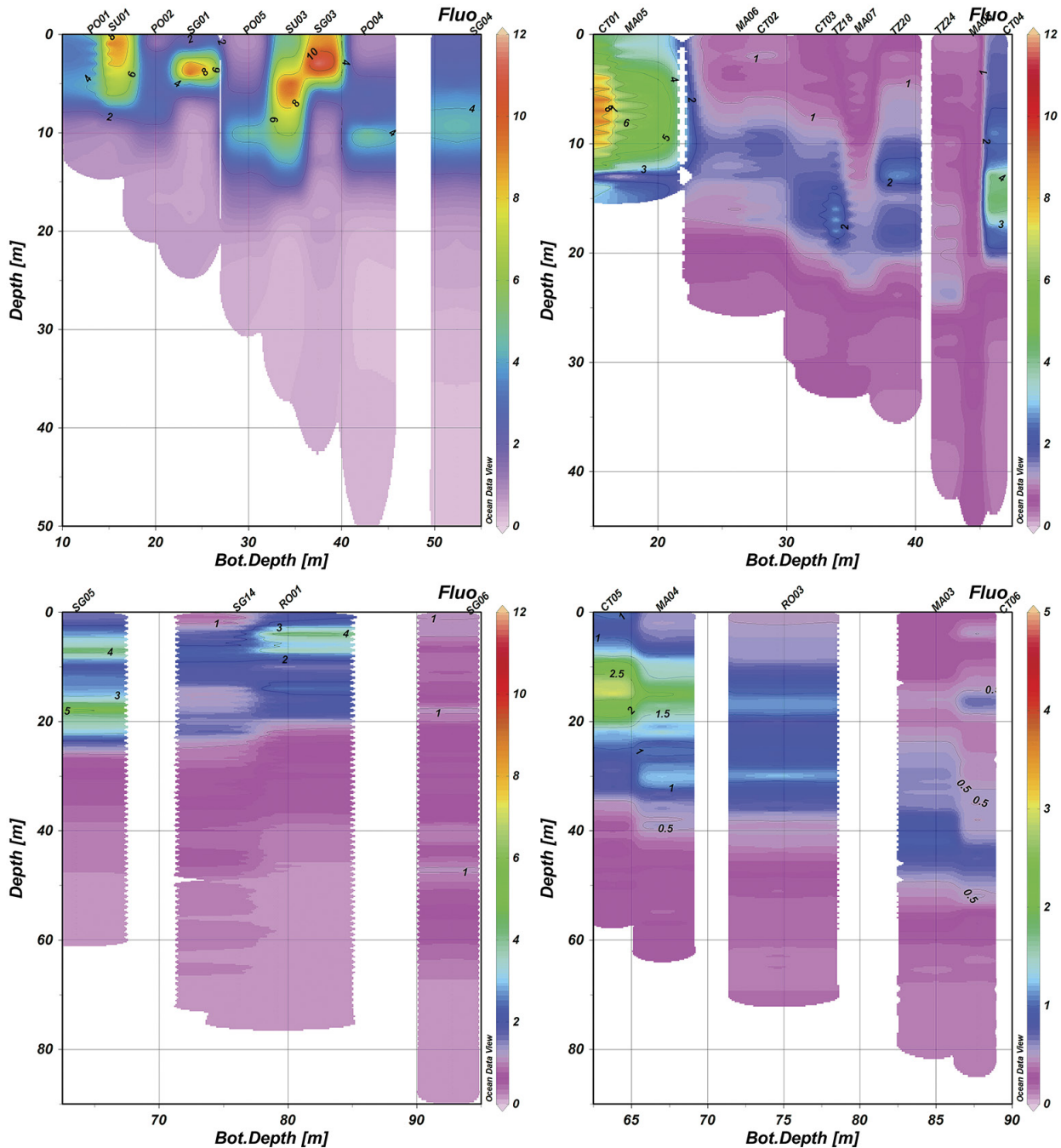


Fig. 9. CTD fluorescence vertical distribution in the studied area (NIS-upper left; SIS-upper right; NOS-lower left; SOS-lower right)

as the shallowest water sample taken at each station, which was always within 5 m of the sea surface (Brown *et al.*, 2015).

The chlorophyll *a* profiles within NIS showed maxima either at the surface layer (at stations SU01 – 17.25 $\mu\text{g}\cdot\text{L}^{-1}$, SG01 – 8.98 $\mu\text{g}\cdot\text{L}^{-1}$, SG03 – 14.30 $\mu\text{g}\cdot\text{L}^{-1}$, PO01 – 4.58 $\mu\text{g}\cdot\text{L}^{-1}$) and PO02 – 3.68 $\mu\text{g}\cdot\text{L}^{-1}$) or at the upper part of thermocline (up to 10 m depth), at deeper stations (Fig. 10). Chl *a* concentrations in SCM ($\text{Chl}_{\text{max } a}$) showed values within 3.10–8.17 $\mu\text{g}\cdot\text{L}^{-1}$, but the M-W test suggests a less developed SCM in accordance with no significant differences observed between the surface Chl *a* and $\text{Chl}_{\text{max } a}$ ($p=0.251$).

Similar to NIS, the Chl *a* concentrations within SIS exhibited the highest values either at surface layer (CT01 – 11.93 $\mu\text{g}\cdot\text{L}^{-1}$, CT02 – 2.92 $\mu\text{g}\cdot\text{L}^{-1}$, and MA05 – 0.78 $\mu\text{g}\cdot\text{L}^{-1}$) or within thermocline. The depth of SCM increased seawards from ~10 m at stations MA06 ($\text{Chl}_{\text{max } a}=0.78 \mu\text{g}\cdot\text{L}^{-1}$) to 20–24 m at stations MA07 ($\text{Chl}_{\text{max } a}=0.74 \mu\text{g}\cdot\text{L}^{-1}$), MA08 ($\text{Chl}_{\text{max } a}=0.38 \mu\text{g}\cdot\text{L}^{-1}$), and TZ 24 ($\text{Chl}_{\text{max } a}=0.27 \mu\text{g}\cdot\text{L}^{-1}$). Anyway, the SCM is better pronounced in SIS than in NIS (Fig 10).

NOS waters exhibited two weak developed subsurface chlorophyll maxima (excepting EuxRO01, where no maximum was found) at different depths. The upper maximum

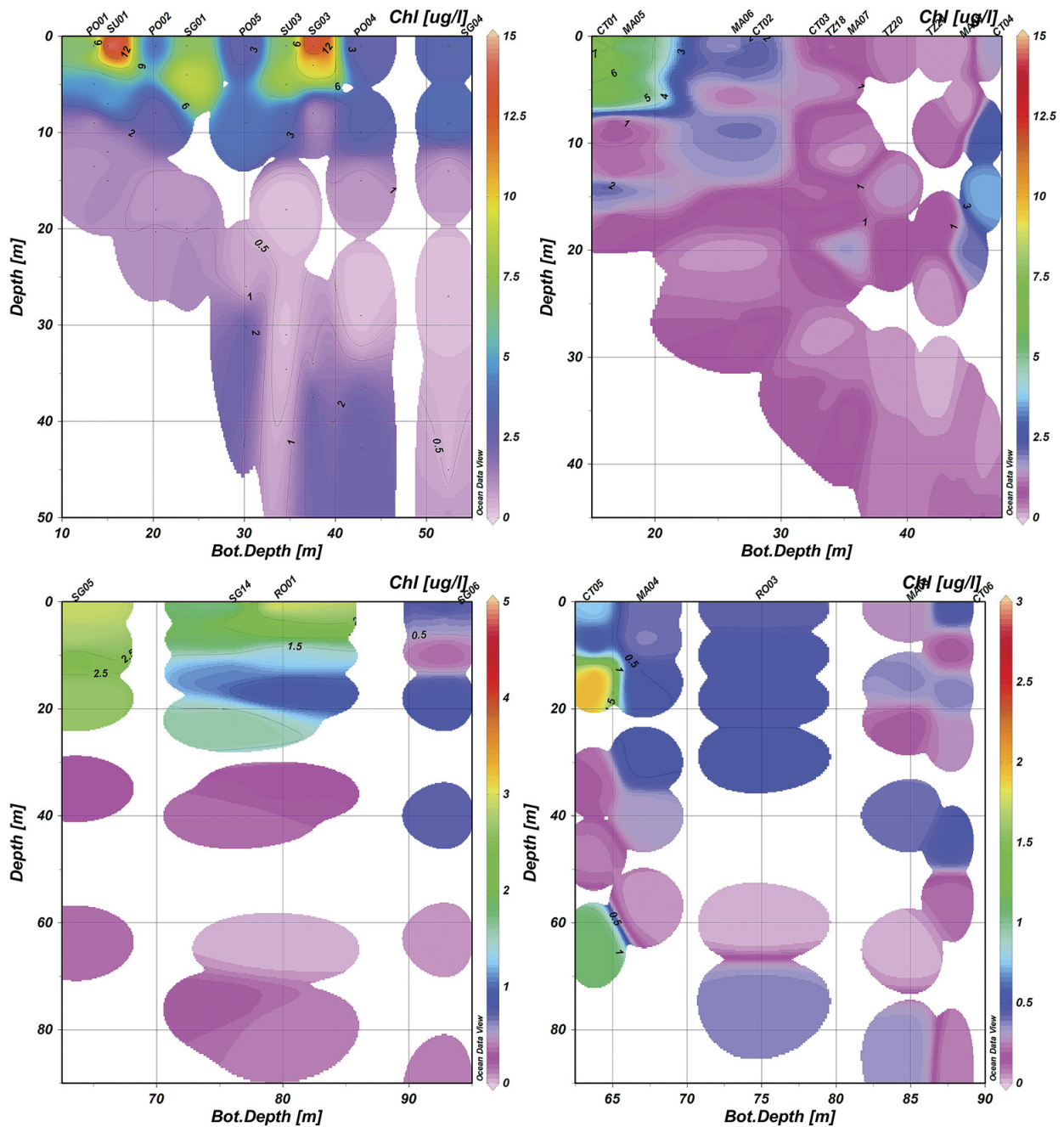


Fig. 10. Chl *a* vertical distribution in the studied area (NIS-upper left; SIS-upper right; NOS-lower left; SOS-lower right)

was observed at the upper part of thermocline, at depths increasing seawards, from 7–9 m at stations SG05 (Chl *a*=2.60 $\mu\text{g}\cdot\text{L}^{-1}$) and SG14 (Chl *a*=1.56 $\mu\text{g}\cdot\text{L}^{-1}$) to 18 m at station SG06 (Chl *a*=0.58 $\mu\text{g}\cdot\text{L}^{-1}$). The deeper maximum was observed at lower part of thermocline, from 18–22 m depth at stations SG05 (Chl *a*=2.63 $\mu\text{g}\cdot\text{L}^{-1}$) and SG14 (Chl *a*=1.66 $\mu\text{g}\cdot\text{L}^{-1}$) up to ~40 m (base of euphotic zone) at deepest station SG06 (Chl *a*=0.52 $\mu\text{g}\cdot\text{L}^{-1}$) (Fig. 10). However, both chlorophyll subsurface maximum layers showed their concentrations smaller than surface Chl *a* (SG05 – 2.89 $\mu\text{g}\cdot\text{L}^{-1}$, SG14 – 1.88 $\mu\text{g}\cdot\text{L}^{-1}$, and SG06 – 0.70 $\mu\text{g}\cdot\text{L}^{-1}$).

Similarly, SOS waters showed two subsurface maxima, excepting for the shallowest station CT05, where only one maximum (Chl *a*=1.98 $\mu\text{g}\cdot\text{L}^{-1}$) was observed at 15 m depth. However, the upper maximum was found at 16–18 m (coinciding with the 15°C isotherm), while the lower one at 30–45 m depths, at the base of euphotic zone (Fig. 10). Chl *a* concentrations measured in both maximum layers were quite close and, generally, showed slight higher values than the surface Chl *a* (contrary to NOS).

As regarding the phaeopigments, a subsurface Phaeo *a* maximum (SPM) was observed in the inner shelf waters (Fig. 11).

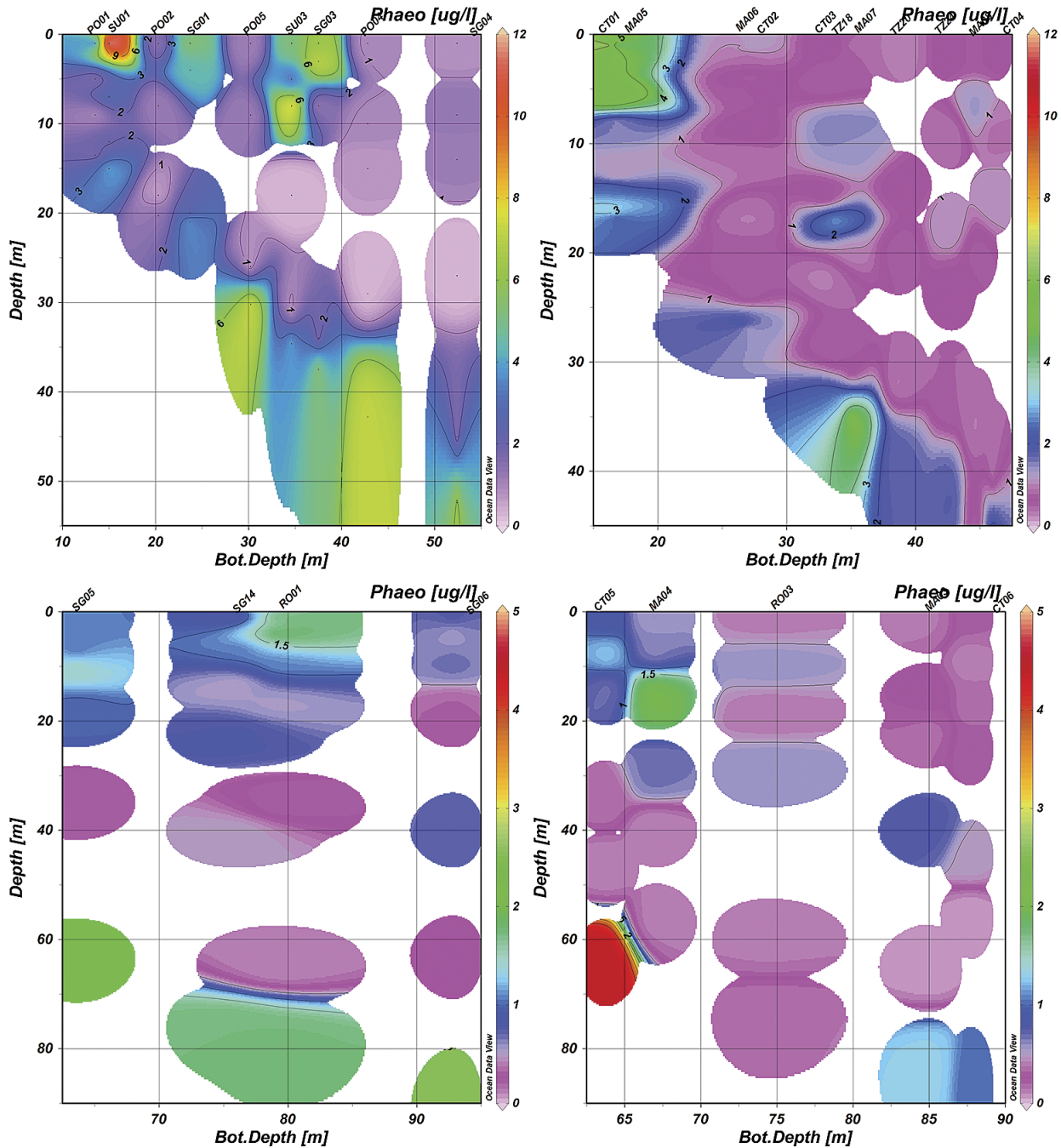


Fig. 11. Phaeo *a* vertical distribution (NIS-upper left; SIS-upper right; NOS-lower left; SOS-lower right)

The stations with the highest Chl *a* concentrations at the surface layer showed the phaeopigments maximum also at sea surface, either within NIS (SU01 – 14.05 $\mu\text{g}\cdot\text{L}^{-1}$, SG01 – 5.32 $\mu\text{g}\cdot\text{L}^{-1}$, SG03 – 7.02 $\mu\text{g}\cdot\text{L}^{-1}$, and PO02 – 1.37 $\mu\text{g}\cdot\text{L}^{-1}$) or SIS (CT01 – 8.58 $\mu\text{g}\cdot\text{L}^{-1}$ and CT02 – 0.85 $\mu\text{g}\cdot\text{L}^{-1}$). The SPM was observed at depths generally coinciding with SCM (6–10 m), but there were two exceptions when the SPM was located just below SCM (at 8 m depth as compared to 6 m, at station SU03) or above it (at 7 m depth as compared to 15m, at station MA08). Phaeo_{max} *a* was lower than Chl_{max} *a*, varying from 0.61 $\mu\text{g}\cdot\text{L}^{-1}$ (TZ20) to 7.82 $\mu\text{g}\cdot\text{L}^{-1}$ (SU03). Below SPM, the Phaeo *a* concentrations decreased gradually up to bottom waters, where they showed significant higher values (Fig. 11). Thus, excepting for the stations with bottom depths <30 m from the northern part of the studied area (SU01, SG01, PO01, and PO02) and in front of Constanta harbor (CT01 and CT02), the highest Phaeo *a* concentrations were measured at the water–sediment interface (maxima on SG04 – 7.69 $\mu\text{g}\cdot\text{L}^{-1}$, PO05 – 7.63 $\mu\text{g}\cdot\text{L}^{-1}$, and PO04 – 7.18 $\mu\text{g}\cdot\text{L}^{-1}$).

As regarding the outer shelf waters, the SPM generally coincided either with the upper chlorophyll maximum (stations SG14 and MA04) or the lower one (stations SG06, CT06, EuxRO03, and MA03), showing Phaeo_{max} *a* between 0.57 $\mu\text{g}\cdot\text{L}^{-1}$ (EuxRO03) $\mu\text{g}\cdot\text{L}^{-1}$ (SG06) and 1.57 $\mu\text{g}\cdot\text{L}^{-1}$ (Ma04) (Fig. 11). Nevertheless, there are 2 exceptions; the first one observed at station SG05 (Phaeo_{max} *a*=1.46 $\mu\text{g}\cdot\text{L}^{-1}$), where SPM is located between the two subsurface chlorophyll maxima and station CT05 (Phaeo_{max} *a*=1.22 $\mu\text{g}\cdot\text{L}^{-1}$), where SPM was shallower than the chlorophyll subsurface maximum (SPM depth=8 m as against SCM depth=15 m). Below the SPM, the phaeopigments in the outer shelf waters showed similar vertical profiles as inner shelf waters, with the highest concentrations at the sediment–water interface (maxima at stations CT05 – 4.40 $\mu\text{g}\cdot\text{L}^{-1}$, SG05 – 2.11 $\mu\text{g}\cdot\text{L}^{-1}$, and SG06 – 2.53 $\mu\text{g}\cdot\text{L}^{-1}$) (Fig. 11).

3.4. MESOZOOPANKTON

Qualitative structure

A total of 23 taxa were found in the area during the investigated period. Overall, the mixotroph dynophlagellate *N. scintillans* dominated the Romanian shelf, making up more than 28% and 49% of the total zooplankton density and biomass, respectively. Usually, *N. scintillans* gives successive blooms starting with April until August, when weather conditions are favourable (Porumb, 1992). The studied period was characterized by an intense process of degradation of *Noctiluca's* cells along with the beginning of a new cycle of flourishing. It attained the maxima of density and biomass at stations PO05 (7,513 ind.m⁻³ and 601 mg.m⁻³) and SG 14 (6,151 ind.m⁻³ and 492.1 mg.m⁻³). Generally, its distribution was uneven, with density and biomass means of 1,462±1,748.1 ind.m⁻³ and 117±1398 mg.m⁻³.

Other dominant taxa after abundance were the larvae of bivalves, barnacles and polychaets (43.6 % as density and 21% as biomass), which attained the greatest abundances

and biomasses in the very coastal area, both in NIS (in average 898.2 ind.m⁻³ and 21.4 mg.m⁻³) and SIS (664.7 ind.m⁻³ and 19.6 mg.m⁻³), as against the deeper stations (36.9 ind.m⁻³ and 2.8 mg.m⁻³ in NOS and 23.0 ind.m⁻³ and 0.1 mg.m⁻³ in SOS, respectively).

The copepods reached 28% and 31% of total zooplankton population as abundance and biomass, out of which *Acartia clausi* represented about 70% and 17%, respectively. *Pseudocalanus elongatus* reached the highest biomass with almost 73%. In total, the copepods were represented by 10 species, among which 2 accidentally freshwater species found in the Sf. Gheorghe area.

Quantitative parameters

Mesozooplankton total density and biomass ranged within 793.9–22,372.2 ind.m⁻³ and 10.7–667.7 mg.m⁻³. Maxima were recorded in stations CT01 and SG14, while minima were measured in stations MA07 and CT03. The K-W test revealed no significant differences between subareas in terms of mesozooplankton total density ($p=0.553$) and total biomass ($p=0.38$).

Within NIS, the mesozooplankton community showed total densities and biomasses from 994 ind.m⁻³ (bivalves larvae and *N. scintillans* accounted for 46% and 33%, respectively) and 35.9 mg.m⁻³ (*N. scintillans* - 74 %), respectively (at shallow station PO02) to 13,474 ind.m⁻³ (*N. scintillans* - 68 % of total density) and 634 mg.m⁻³ (*N. scintillans* - 98 % of total biomass), respectively (PO05). Generally, the density and biomass decreased progressively seaward from 5,571.5 ind.m⁻³ and 458.2 mg.m⁻³, respectively, at the shallowest station SG 01 to 2,261.8 ind.m⁻³ and 261.7 mg.m⁻³, respectively, at the edge of the inner shelf (SG04). Only in the Portita bay, there were found higher values at deeper stations (PO 04 and PO 05), most likely in connection with the upwelling process.

Within SIS, the total densities and biomasses varied largely from 793.9 ind.m⁻³ (MA07 - *N. scintillans* and bivalves larvae were dominant with 68.5% and 20.6 %, respectively) and 10.7 mg.m⁻³ (CT03 - *N. scintillans* with 40 % and bivalves larvae with 22 % were dominant), respectively to 22,372.2 ind.m⁻³ (CT01 - *Amphibalanus improvisus* with 47 %, bivalves larvae with 32 %, and *Acartia* sp. with 19 % were dominant) and 324.4 mg.m⁻³ (TZ20 - *N. scintillans* was the dominant species with 97 % of total biomass), respectively. Although a decline in zooplankton abundance was also observed seaward, both in the Constanta and Mangalia areas, it is noteworthy the high density found at CT 04 (2,947.3 ind.m⁻³) strongly linked to lower SSS (favouring higher surface Chl *a* and Chl_{max} *a*). This observation is supported by the significant correlations of total density with SSS ($r=-0.612$, $p=0.002$) and surface Chl *a* ($r=0.41$, $p=0.004$) and no significant correlations found between total density and bottom depths. As regarding the biomass, no significant relationships with SSS and bottom depths were observed, thus suggesting a patchy distribution depending on the qualitative structure.

Higher densities and biomasses within NOS were measured at SG14 (7,367.6 ind·m⁻³ and 667.7 mg·m⁻³, respectively) as compared to stations EuxRO01 (2,624 ind·m⁻³ and 228.2 mg·m⁻³, respectively) and SG06 (1,307.3 ind·m⁻³ and 86.4 mg·m⁻³, respectively). Within SOS, the zooplankton distribution in terms of total density was quite homogeneous (1,625.3–2,069.6 ind·m⁻³; CV=12 %). On contrary, the total biomasses showed a greater variability (139.6–446.2 mg·m⁻³; CV=62 %), mainly due to the highest value recorded at station EuxRO03

4. DISCUSSIONS

4.1. SPATIAL DISTRIBUTION OF CHL *a* AND PHAEO *a*

The surface Chl *a*, surface Phaeo *a*, Chl_{max} *a* and Phaeo_{max} *a*, SCM depth and SPM depth are the parameters used in the present paper to characterize the chlorophyll and phaeopigments regimes.

As is mentioned above, significant differences were observed between subareas in terms of surface Chl *a* and Phaeo *a*, but it's noteworthy as well the large variability of both parameters observed within each subareas (CVs=39–143.4% and 34.1–184.2%), particularly in the inner shelf waters (CV_{NIS}=78.7% and 107.0%; CV_{SIS}=143.4% and 184.2%). The highest CVs within SIS are mainly due to the considerable high surface Chl *a* in station CT01 (Fig. 8), while within NIS, the large variability resulted either from the larger nutrient-rich freshwater input from the Danube which provided optimal conditions for phytoplankton development and thus an increased grazing pressure or the coastal upwelling processes (colder and more saline surface waters) which led to less intense algal growth and lower grazing pressure. This can be linked with higher mesozooplankton total density found in the Danube's mouths area and, on the other side, the lower densities measured at shallower stations in the Portita bay. Similarly, higher mesozooplankton total density was found at station CT01 (SSS=9.62 PSU), while the lowest one at station MA07 (SSS=17.77 PSU).

The K-W tests applied to variables Chl_{max} *a* and Phaeo_{max} *a*, SCM depth, SPM depth showed significant differences between the subareas in terms of Chl_{max} *a* (p=0.001), SCM depth (p=0.021), and SPM depth (p=0.025), and no significant differences for Phaeo_{max} *a*. Thus, NIS waters showed significant shallower SCM and higher Chl_{max} *a* as compared to SIS, NOS, SOS. SIS waters exhibited shallower SCM and higher Chl_{max} *a* as compared to SOS (Table 3).

The surface Chl *a* has a major influence on the subsurface Chl *a* growth environment by altering the penetration of light and determining the phytoplankton to rise/accumulate at shallower depths (Brown *et al.*, 2015). This is in accordance with the significant relationships established between surface Chl *a* and SSS with Chl_{max} *a* (r=-0.637, p=0.001 and r=-0.637, p<0.0001, respectively) and SCM depth (r=0.432, p=0.045 and r=-0.637, p<0.0001 and r=0.432, p=0.045), re-

spectively, which explain the shallowest SCM having highest Chl_{max} *a* within NIS. The larger runoff from the Danube provided optimal conditions for the algal growth within NIS which led to phytoplankton rising/accumulation at shallower depths, thus showing a SCM at depths within 5–10 m (Figs. 9 and 10). Some stations within SIS (CT04, TZ18, TZ20, TZ24, and MA08) showed the SCM at depths corresponding with the subsurface DO maximum layer, thus suggesting intense photosynthetic process.

The influence of hydrological regime on the chlorophyll vertical variability was significant in the outer shelf waters as well; a second chlorophyll maximum, generally shallower than the true SCM, was observed at the upper part of thermocline (Figs. 9 and 10). Within NOS, the upper chlorophyll maximum deepened seawards from 7–8 m (SG05 and SG14) to 19–20 m (SG06). At the deepest station SG06, the upper chlorophyll maximum coincided with the DO subsurface maximum suggesting relatively intense photosynthetic processes, while at shallower stations, SG05 and SG14, DO values corresponding to upper chlorophyll maximum were quite similar to those recorded at the surface layer. Thus, the latter chlorophyll maxima can be the result of cell accumulation on seasonal upper pycnocline (Raimbault *et al.*, 1993), contrary to deeper waters where the upper chlorophyll maximum is most likely linked to the primary production.

The SOS waters showed also a shallower chlorophyll maximum (excepting for the shallowest and deepest stations, CT05 and MA03, respectively) at depths of 15–18 m (Figs. 9 and 10). Similar to the deepest station of NOS (SG06), the upper chlorophyll maximum coincided with the DO maximum, thus it can be associated to primary production.

The deeper SCM (located at the base of euphotic zone) were observed both in NOS and SOS (30 – 45 m depth) and most likely is linked to the photoacclimation of phytoplankton. Steele (1964), supported by Fennel & Boss (2003), suggested that in nutrient low waters (PO₄=0.002–0.18 μM; NO_x=0.59–0.94 μM; NH₄=0.27–0.95 μM), the SCM can not be associated with an increase in biomass, but rather with an increase in the chlorophyll per biomass at low light levels.

The upper chlorophyll maxima were slight smaller or very close to Chl_{max} *a* (0.77 ± 0.83 μg·L⁻¹ as compared to 0.88 ± 0.88 μg·L⁻¹). Similar to Chl_{max} *a*, the upper chlorophyll maximum showed a significant negative correlation with SSS (r=-0.855, p=0.014), thus stronger upper maximum were measured within NOS (highest concentrations at stations SG05 – 2.60 μg·L⁻¹ and SG14 – 1.59 μg·L⁻¹), where SSS showed significant lower values than SOS (Table 2).

The phaeopigments vertical distribution showed maxima generally at depth corresponding to SCM as it is suggested by the significant positive correlation between SCM depth and SPM depth (r=0.776, p<0.0001). Significant shallower SPM depth were observed within NIS as compared to NOS and SOS (Table 3). Contrary to SCM depth, no significant differences were observed between NIS and SIS in terms of SPM

depth as a result of shallower SPM found at stations MA07 and MA 08 as compared to SCM depth. Most likely, the presence of SPM just below the upper layer is due to grazing processes within the upper layer resulting in the release of phaeopigments in fecal material by micrograzers (Stoecker, 1984) and their accumulation at the upper boundary of seasonal pycnocline (very close to the surface layer, 7–8 m depth). Similar situations were also found within both NOS and SOS, at stations SG05, SG14 and MA04, where the SPM was shallower (7–8 m depth) and coincided with the upper chlorophyll maximum. In these stations, the phaeopigments vertical profiles showed a second maximum (Fig. 11), but contrary to chlorophyll where the deeper maximum was considered as true SCM, the deeper phaeopigments maximum (0.48–0.96 $\mu\text{g}\cdot\text{L}^{-1}$) is considerable less developed than the shallower one (0.96–1.97 $\mu\text{g}\cdot\text{L}^{-1}$) (Fig. 11). Thus, in above mentioned situations, we considered the shallower phaeopigments maximum as true SPM.

The remaining phaeopigments' measurements performed in the inner shelf waters showed the SPM depth coinciding with SCM depth. This is in accordance with Soo-Hoo & Kiefer (1982) who suggest that fecal particles containing phaeopigments are so small that their sinking velocities are negligible and are subject to photodegradation. Thus, the concentration of phaeopigment at a given depth results from a balance between local rates of grazing and rates of photooxidation (Soo-Hoo & Kiefer, 1982). Most likely, the grazing pressure is so high at SCM depth that the phaeopigments displayed their maxima at the same depth.

In terms of Phaeo_{max} *a* (within 0.28–2.71 $\mu\text{g}\cdot\text{L}^{-1}$; with minimum at station CT06 and maximum at station TZ18), no significant differences were found between subareas. The significant negative correlation established between SPM depth and Phaeo_{max} *a* suggests higher Phaeo_{max} *a* at shallower SPM, that can be related either to higher grazing pressures at those depths or photodegradation of sinking fecal particles. Unlike the surface Phaeo *a*, significantly correlated with mesozooplankton density ($r=0.55$, $p=0.003$), no significant correlations between SPM and Phaeo_{max} *a* and mesozooplankton density were established.

Phaeopigments concentrations decrease below SPM up to the bottom waters, generally reaching maxima at water-sediment interface (Fig. 11). Higher phaeopigments concentrations at the water-sediment interface are most likely related to chlorophyll degradation products in senescent phytoplankton and detritus settled on the sediment surface (Herbland, 1988). The K-W test applied for the Chl/Phaeo ratio at water-sediment interface showed significant differences between subareas ($p=0.048$). The ratios found within inner shelf waters (both NIS and SIS) displayed significant higher values than those within NOS (M-W, $p=0.009$ and M-W, $p=0.026$, respectively), suggesting larger amounts of fresh (i.e. not degraded) Chl *a* in bottom waters that correspond to the recently produced organic matter (in the same season)

rather than re-suspended from shelf sediments, according to Brown *et al.* (2015). This can be linked with higher surface Chl *a* and Chl_{max}*a* concentrations (suggesting higher primary production) measured especially within NIS, but also in SIS.

4.2. RELATIONSHIPS BETWEEN CHLOROPHYLL PRODUCTS AND ZOOPLANKTON COMMUNITY

The present study investigated whether a relationship between the chlorophyll pigments and abundances of dominant zooplankton taxa could be accounted for the distributional pattern observed. Although a direct relation based on the pigments' gut content or their presence in faecal pellets of the zooplankton species has not been analysed, some preliminary conclusions on the preferences of zooplankton species for different environmental variables, including the trophic condition of the areas, were drawn.

A non-parametric Kendall's tau rank correlation coefficient was performed in order to reveal the relationships of different taxa with the environmental factors in the area, especially the Chl *a* and Phaeo *a*. Hence, statistically significant positive correlations ($r=0.68$, $p<0.0001$ and $r=0.67$, $p<0.0001$, respectively) of bivalves' larvae, nauplia of *Amphibalanus improvisus* and *Acartia* sp. abundances with surface Chl *a* and Phaeo *a* were noted. The polychaets larvae were also positively correlated with surface Chl *a* and Phaeo *a* ($r=0.64$, $p=0.037$ and $r=0.62$, $p=0.017$, respectively). In turn, negative relations of copepod *Paracalanus parvus* with the surface Chl *a* and Phaeo *a* ($r=-0.65$, $p=0.002$ and $r=-0.57$, $p=0.017$, respectively) were identified, while *N. scintillans* showed no significant correlations with any of the above. In terms of biomass, the bivalves' larvae were positively correlated with surface Chl *a* and Phaeo *a* ($r=0.69$, $p<0.0001$ and $r=0.66$, $p=0.004$, respectively), while the polychaets larvae showed a positive correlation only with the former ($r=0.61$, $p=0.005$). Many studies (Abe *et al.*, 2011; Almeda *et al.*, 2009) revealed that the meroplankton, which dominated by far the coastal waters, have a major impact on the structure of phytoplankton (chlorophyll) during the blooming periods. Analysing the vertical distribution and feeding of bivalve veligers in stratified waters, Raby *et al.* (1994) showed that the fullest larvae are in the same layer as the maximum Chl *a* is located, which, in case of the present study, was found either in the surface layer or at upper part of thermocline. Thus, the shallower stations SU01 and CT01 (high concentrations of Chl *a*) were populated by large communities of bivalve veligers. The barnacles' nauplia formed also large agglomerations in shallow waters mainly as a result of intense reproduction period of genitors living on the natural or artificial hard substrate in the coastal area. *A. improvisus* abundances were positively correlated with chlorophyll and phaeopigments, indicating its preferences for eutrophic environments, which supported their high proliferation (Nasrolahi *et al.*, 2007).

N. scintillans was not significantly correlated with surface Chl *a* and Phaeo *a*, in accordance with different studies (Huang & Qi, 1997; Miyaguchi *et al.*, 2006; Turkoglu, 2012).

Among the copepods, only *Acartia* sp. and *P. parvus* were significant correlated with the chlorophyll pigments. *Acartia* sp. density showed significant positive correlations with surface Chl *a* and Phaeo *a*, while *P. parvus* showed negative correlations. Both species are mainly known as active phytoplankton filter feeders (Benedetti *et al.*, 2016) though evidences for a supplementary raptorial feeding mode were also documented (Katechakis *et al.*, 2004). According to Katechakis *et al.* (2002), *A. clausi* decreases its filtration efforts at higher food concentrations though it maintains the ingestion rates at a stable level, while the gut evacuation rate increases with food concentration, especially diatoms (Tirelli & Mayzaud, 2005). Chl *a* seems to be important during critical life stages (egg production) of *P. parvus* (Uye & Shibuno, 1992). However, no positive correlation between *P. parvus* abundances and surface Chl *a* was found as it was documented by Jang *et al.* (2010).

CONCLUSIONS

The physical processes such as the large runoff from the Danube River and the coastal upwelling phenomenon, altogether with the complex biological dynamics (responses to light, nutrients and grazing, etc.) strongly contributed to high spatial variability of Chl *a* and Phaeo *a* distribution in the studied area (either in the surface layer or water column).

Surface Chl *a* and Phaeo *a* showed a large spatial variability, with the highest concentrations within NIS (especially in the Danube's mouths area), but also high surface Chl *a* was observed within NOS (significant higher than SIS and SOS), strongly linked to the Danube's large freshwater discharge. The vertical profiles of Chl *a* in the inner shelf waters showed a subsurface maximum at depths ranging from 6 m to 24 m,

shallower (<10 m) and stronger within NIS, in accordance with the lower SSS. The outer shelf waters generally showed the SCM at depths corresponding to the base of euphotic zone (30–45 m), most likely linked to the photoacclimation of phytoplankton. Most of stations within NOS and SOS were characterized by the presence of a second chlorophyll layer, shallower (7–20 m depth) and slight weaker than SCM, generally coinciding with the DO subsurface maximum (intense photosynthetic processes). The phaeopigments vertical distribution showed also a subsurface maximum, generally at depth corresponding to SCM. Below SCM, Phaeo *a* concentrations decreased up to the bottom waters, where there was observed a considerable increase (sometimes reaching maxima at water-sediment interface).

The zooplankton populations were characterized by high densities and biomasses predominantly in the very coastal stations (both in NIS and SIS), which decreased significantly seawards (NOS and SOS). The qualitative structure was dominated by the copepods species (10 species), while *N. scintillans* and the meroplankton representatives (polychaets, barnacles and bivalves larvae) made up more than 80% of the total abundances. In the late spring/early summer, the meroplankton plays an important role in controlling the abundances of phytoplankton stocks, the chlorophyll products spatial distribution, mainly in the coastal waters.

ACKNOWLEDGEMENTS

The present study has been supported by the Ministry of Research and Innovation within the framework of the Nucleus Program, the project PN16 45 01 01 – Geo-ecological monitoring of the Romanian Black Sea shelf.

REFERENCES

- ABE, H., SATO-OKOSHI, W., ENDO, Y., (2011). Seasonal changes of planktonic polychaete larvae and chlorophyll *a* concentration in Onagawa Bay, northeastern Japan, *Italian Journal of Zoology*, **78**, suppl. 1, 255–266
- ALEXANDROV, B., ARASHKEVICH, E., GUBANOVA, A., KORSHENKO, A., (2014). Black Sea Monitoring Guidelines. Mesozooplankton, EU/UNDP Project: *Improving Environmental Monitoring in the Black Sea-EMBLAS*, www.emblas.org
- ALMEDA, R., PEDERSEN, T.M., JAKOBSEN, H.H., ALCARAZ, A., CALBET, A., HANSEN, B.W., (2009). Feeding and growth kinetics of the planktotrophic larvae of the spionid polychaete *Polydora ciliata* (Johnston), *J. Exp. Mar. Biol. Ecol.*, **382**, 61–68
- AMINOT, A., REY, F., (2001). Chlorophyll *a*: determination by spectroscopic methods, *ICES Tech. Mar. Environ. Sci.*, **30**, 1-18
- BENEDETTI, F., GASPARINI S., AYATA, S-D., (2016), Identifying copepod functional groups from species functional traits, *J. Plankton Res.*, **38**, 1, 159–166
- BOLOGA, A.S., (1977). The phytoplankton assimilatory pigments along the Romanian coast of the Black Sea during 1976, *Recherches Marines*, **10**, 95-107
- BOLOGA, A.S., (1978). The monthly dynamics of phytoplanktonic assimilatory pigments from the sector Constanta-Agigea of the Romanian Black Sea coast during 1977, *Recherches Marines*, **11**, 77–83
- BOLOGA, A.S., BURLAKOVA, Z.P., TCHMYR, V.D., KHOLODOV, V.I., (1985). Distribution of chlorophyll *a*, phaeophytin *a* and primary production in the Western Black Sea (May 1982), *Recherches Marines*, **18**, 97-115
- BROWN, Z.W., LOWRY, K.E., PALMER, M.A., VAN DUJEN, G.L., MILLS, M.M., PICKART, R.S., ARRIGO, K.R., (2015). Characterizing the subsurface chloro-

- phyll a maximum in the Chukchi Sea and Canada Basin, *Deep-Sea Research II*, **118**, 88 – 104
- CHU, P.C., IVANOV, L.M., MARGOLINA, T.M., (2005). Seasonal variability of the Black Sea chlorophyll a concentration, *Journal of Marine Systems*, **56** (3-4), 243-261
- CULLEN, J.J., (1982). The deep chlorophyll maximum: comparing vertical profiles of chlorophyll a, *Canadian Journal of Fisheries and Aquatic Sciences*, **39**, 791–803
- DEMIDOV, A.B., (2008). Seasonal dynamics and estimation of the annual primary production of phytoplankton in the Black Sea, *Oceanology*, **48** (5), 664-678
- FALKOWSKI, P.G., KOLBER, Z., (1995). Variations in Chlorophyll fluorescence yields in phytoplankton in the world oceans, *Aust. J. Plant Physiol.*, **22**, 341–355
- FENNEL, K., BOSS, W., (2003). Subsurface maxima of phytoplankton and chlorophyll: Steady-state solutions from a simple model, *Limnol. Oceanogr.*, **48**(4), 1521–153
- GRASSHOFF, K., KREMLING, K., EHRHARDT, M., (1999). *Methods of Seawater Analysis*. 3rd Edition, Weinheim, Wiley-VCH, 632 pp.
- HANSON, C.E., PESANT, S., WAITE, A.M., PATTIARATCHI, C.B., (2007). Assessing the magnitude and significance of deep chlorophyll maxima of the coastal eastern Indian Ocean, *Deep-Sea Research II*, **54**, 884 – 901
- HERBLAND, A., (1988). The deep phaeopigments maximum in the ocean: reality or illusion?, in: Rothschild, B., J. (ed.) *Toward a theory on biological-physical interactions in the world ocean*, Amsterdam: Kluwer Academic, 157-172
- HUANG, C., QI, Y., (1997). The abundance cycle and influence factors on red tide phenomena of *Noctiluca scintillans* (Dinophyceae) in Dapeng Bay, the South China Sea, *J. Plankton Res.*, **19**, 303–318
- JANG, M.-C., SHIN, K., LEE, T. ET AL., (2010). Feeding selectivity of calanoid copepods on phytoplankton in Jangmok Bay, south coast of Korea, *Ocean Sci. J.*, **45**, 101–111
- JEFFREY, S.W., (1980). Algal pigment systems, in: Falkowski, P.G., (ed.), *Primary productivity in the sea*, Plenum, New York, p. 33-58
- KATECHAKIS, A., STIBOR, H., SOMMER, U. ET AL., (2002). Changes in the phytoplankton community and microbial food web of Blanes Bay (Catalan Sea, Mediterranean) under prolonged grazing pressure by doliolids (Tunicata), cladocerans or copepods (Crustacea), *Mar. Ecol. Prog. Ser.*, **234**, 55–69.
- KATECHAKIS, A., STIBOR, H., SOMMER, U., HANSEN, T., (2004). Feeding selectivities and food niche separation of *Acartia clausi*, *Penilia avirostris* (Crustacea) and *Doliolum denticulatum* (Thaliacea) in Blanes Bay (Catalan Sea, NW Mediterranean), *J. Plankton Res.*, **26**, 589–603
- KRUPATKINA, D.K., FINENKO, Z.Z., SHALAPYONOK, A.A., (1991). Primary production and size-fractionated structure of the Black Sea phytoplankton in the winter-spring period, *Mar. Ecol. Prog. Ser.*, **73**, 25 – 31
- LORENZEN, C.J., (1967). Vertical distribution of chlorophyll and phaeopigments: Baja California, *Deep Sea Res.*, **14**, 735-745
- MIHNEA, P.E., (1988). Chlorophyll a in the Romanian Black Sea area, *Rapports de la Commission Internationale pour l'Exploration Scientifique de la Mer Méditerranée*, **31**, 2-59
- MIHNEA, P.E., (1997). Major shifts in the phytoplankton community (1980-1994) in the Romanian Black Sea, *Oceanologica Acta*, **20** (1), 119-129
- MIYAGUCHI, H., FUJIKI, T., KIKUCHI T., KUWAHARA V., S., TATSUKI, T., (2006). Relationship between the bloom of *Noctiluca scintillans* and environmental factors in the coastal waters of Sagami Bay, Japan, *J. Plankton Res.*, **28**, 3, 313–324
- NASROLAHI, A., SARI, A., SAIFABADI, S., MALEK, M., (2007). Effects of algal diet on larval survival and growth of the barnacle *Amphibalanus* (= *Balanus*) *improvisus*, *Journal of the Marine Biological Association of the UK*, **87** (05), doi: 10.1017/S0025315407057037
- PORUMB, F., (1992). On the development of *Noctiluca scintillans* under eutrophication of Romanian Black sea waters, *Sci. Tot. Environ.*, **126** (Suppl.), 907–920
- RABY, D., LAGADEUC, Y., DODSON J.J., MINGELBIER, M., (1994). Relationship between feeding and vertical distribution of bivalve larvae in stratified and mixed waters, *Mar. Ecol. Prog. Ser.*, **103**, 275–284
- RAIMBAULT, P., COSTE, B., BOULHADID, M., BOUDJELLAL, B., (1993). Origin of high phytoplankton concentration in deep chlorophyll maximum (DCM) in a frontal region of southwestern Mediterranean Sea (Algerian current), *Deep Sea Res.*, **40**, 791 – 804
- SCHLITZER, R., (2017). Ocean Data View, <http://odv.awi.de>.
- SOO-HOO, J.B., KIEFER, D.A., (1982). Vertical distribution of phaeopigments—II. Rates of production and kinetics of photooxidation, *Deep Sea Research Part A. Oceanographic Research Papers*, **29**, 12, 1553 – 1563
- STEELE, J., (1964). A study of production in the Gulf of Mexico, *J. Mar. Res.*, **3**, 211–222
- STEFANOVA, E., STEFANOVA, K., KOZUHAROV, D.S., (2012). Mesozooplankton Assemblages in Northwestern Part of Black Sea, *Acta zool. bulg.*, **64** (4), 403–412
- STEL'MAKH, I., BABICH I., TUGRUL, S., MONCHEVA, S., STEFANOVA, K., (2009). Phytoplankton Growth Rate and Zooplankton Grazing in the Western Part of the Black Sea in the Autumn Period, *Oceanology*, **49**, 1, 83–92
- STOECKER, D.K., (1984). Particle production by planktonic ciliates, *Limnol. Oceanogr.*, **29**, 930-940
- TAGUCHI, S., LAWS, E.A., BIDIGARE, E.R., (1993). Temporal variability in chlorophyll a and phaeopigment concentrations during incubations in the absence of grazers, *Mar. Ecol. Prog. Ser.*, **101**, 45 – 53
- TIRELLI, V., MAYZAUD, P., (2005). Relationship between functional response and gut transit time in the calanoid copepod *Acartia clausi*: role of food quantity and quality, *J. Plankton Res.*, **27**, 6, 1, 557–568
- TURKOGLU, M., (2012). Red tides of the dinoflagellate *Noctiluca scintillans* associated with eutrophication in the Sea of Marmara (the Dardanelles, Turkey) *Oceanologia*, **55** (3), 709–732
- UYE, S., SHIBUNO, N., (1992). Reproductive biology of the planktonic copepod *Paracalanus* sp. in the Inland Sea of Japan, *J. Plankton Res.*, **14**, 343–358.

- VASILIU, D., LAZAR, L., GOMOIU, M.-T., TIMOFTE, F., (2010 a). Recent data concerning on vertical distribution of chlorophyll *a* in the Western Black Sea, *Recherches Marines*, **39**, 109-123
- VASILIU, D., GOMOIU, M.-T., BOICENCO, L., LAZAR, L., TIMOFTE, F., (2010 b). Chlorophyll *a* distribution in the Romanian Black Sea inner shelf waters in 2009, *Geo-Eco-Marina*, **16**, 19–28
- VASILIU, D., BOICENCO, L., GOMOIU, M.-T., LAZAR, L., MIHAILOV, M.-E., (2012). Temporal variation of surface chlorophyll *a* in the Romanian near-shore waters, *Med. Mar. Sci.*, **13/2**, 213-226
- VELIKOVA, V., COCIAȘU, A., POPA, L., BOICENCO, L., PETROVA, D., (2005). Phytoplankton community and hydrochemical characteristics of the Black Sea, *Water Science and Technology*, **51**, 11, 9-18
- WOLKEN, J.J., MELLON, A.D., GREENBLATT, C.L., (1955). Environmental factors affecting growth and chlorophyll synthesis, *J. Protozool.*, **2**, 89 – 96
- YENTSCH, C.S., (1965). Distribution of chlorophyll and phaeophytin in the open ocean, *Deep Sea Res.*, **12**, 653-666
- YUNEV, O.A., (1989). Spatial distribution of chlorophyll *a* and phaeophetin *a* in the western Black Sea in winter, *Oceanologia*, **29**, 480-485 (in Russian)
- YUNEV, O.A., MONCHEVA, S., CARSTENSEN, J., (2005). Long-term variability of vertical chlorophyll *a* and nitrate profiles in the open Black Sea: eutrophication and climate change, *Mar. Ecol. Prog. Ser.*, **294**, 95 – 107
- YUNEV, O.A., CARSTENSEN, J., MONCHEVA, S., KHALILULIN, A., AERTEBJERG, G., NIXON, S., (2007). Nutrient and phytoplankton trends on the western Black Sea shelf in response to cultural eutrophication and climate change, *Estuarine, Coastal and Shelf Science*, **74**, 63-76

